Key Engineering Materials
ISSN: 1662-9795, Vol. 926, pp 1736-1745
doi:10.4028/p-d3uuc2

Submitted: 2021-12-08
Revised: 2022-02-01
Accepted: 2022-02-01
Online: 2022-07-22

Evaluating the Corrosion Resistance of Inconel 625 Coatings, Processed by Compact Plasma Spray, for Applications in Concentrating Solar Power Plants

Felice Rubino[1,a*], David Merino[1,b], Claudio Munez[1,c] and Pedro Poza[1,d]

[1]DIMME – Durability and Mechanical Integrity of Structural Materials, Universidad Rey Juan Carlos, Escuela Superior de Ciencias Experimentales y Tecnología, C/ Tulipán s.n. 28933 Móstoles (Madrid), Spain

[a] felice.rubino@urjc.es, [b]david.merino@urjc.es, [c]claudio.munez@urjc.es, [d]pedro.poza@urjc.es

Keywords: Compact plasma spray, coating, corrosion protection, molten salts, thermal energy storage.

Abstract. Thermal energy storage (TES) systems have paramount importance in the design of Concentrating Solar Power (CSP) plants. TES systems allow storing the energy collected from solar radiation as heat energy in a thermal fluid and, in that way, extending the energy duration period of the plant and making the produced electricity dispatchable, depending on the actual demand and not only on the availability of the sun. The thermal fluids, synthetic oils, or molten salts, usually operate at temperatures from 500°C up to 800°C. The harsh operative conditions bring out issues related to the compatibility with the construction materials of CSP components, i.e., carbon and stainless steel. Coating of low-alloy structural steel with high-resistant materials has been addressed as a promising solution for mitigating the corrosion in TES system components. Compact plasma spray process was used to deposit Inconel 625 alloy onto T22 carbon steel coupons. Nitrate salts mixture, 60%$NaNO_3$-40KNO_3, commonly employed in CSP systems as operative and thermal storage fluid was used as corrosion medium. The tests were conducted by immersing coated and uncoated samples in molten salts at 500°C for 1, 3 7, and 14 days to assess the corrosion behavior of the In625 coatings. After 24 hours of exposition to molten nitrate salts, the T22 surface showed a pronounced oxidized layer having a thickness of approximately 20 μm. This layer is mainly composed of oxygen, iron, and chromium, which are the main constituents of carbon steel, with a few traces of sodium and potassium derived from the reaction of salts with the steel. Inconel 625, on the other hand, showed the formation of very thin scales of corrosion products localized only on the surface of the sample. Longer exposition is expected to produce a more pronounced degradation of uncoated steel, but barely affect the Inconel 625 coating

Introduction

The usage of thermal energy storage (TES) systems in CSP technologies has consolidated in the design of the plants. Their integration with the solar energy harvesting and the power cycle systems, indeed, allows to extend the period of the exploitation of solar energy even during the night hours without the solar radiation, mitigate the short-term variations of sunlight, and make the sun-derived electricity dispatchable [1,2]. The TES systems employ heat thermal fluids to store the energy gathered from the solar receivers as heat at high temperatures [3]. In the last decades, the CSP/TES systems have resorted more and more to molten salts as fluid for the power cycle or heat storage media to operate at very higher temperatures, from the range of 300-500°C up to 800°C [3–5]. However, the construction materials employed within the CSP components, e.g., carbon and stainless steels or, Ni-based super-alloys may suffer from severe corrosion attacks by the molten salts at these temperatures, bringing out challenging issues related to the integrity of these materials and their compatibility with the heat thermal fluids [6,7].

Carbon and low-alloyed steels, such as low-Cr grade T22 steel, A36, and A56 gr.70 grade steel, commonly employed to fabricate the components of CSP and TES systems, provide remarkable corrosion resistance against nitrate salts mixtures (Solar salt and Hitec/Hitec XL system) at low

working temperatures, up to 390-400°C maximum, but above this threshold, higher corrosion rates, and catastrophic failures have been observed [6,8–10]. High resistant materials, such as 304, 310, 316, and 347 stainless steels, or Inconel 625, In800H, and Hastelloy C-276 Ni-based alloys have adopted for CSP technologies to operate at more demanding conditions, although even them can suffer dramatic degradation at temperature above 750/800°C [3]. Several strategies have been proposed in recent years to prevent or mitigate the corrosion-derived damages in storage tanks. These involve the addition of a corrosion inhibitor to the electrolyte, cathodic protection, or the application of protective coatings having better corrosion resistance than the structural materials [11,12]. Coating of low-alloy structural steel represents a suitable and cost-effective alternative in the design of CSP plants. Indeed, the coatings act as protective layers avoiding the oxidation of the elements of the substrate (especially those more prone to the oxidation, such as Cr, Ni, Al, and the depletion of the matrix of its constituents; in that way, they can enhance the lifetime of these materials by sacrificing their element during the usage [13]. In this context, Ni-Cr alloys are very promising systems to be used as protective coatings in harsh environments [14]. Among the proposed strategies to deposit protective coatings on metallic components, thermals spray (TS) techniques have gained a growing interest since the ‘80s, when first attempts have been made to produce thermal barrier and wear-resistant coatings for incinerators, fuel cells, steam tanks, and aeronautic components [15–21]. Ni20Cr coatings deposited by High-Velocity Oxygen Fuel (HVOF) and combustion powder spray processes have been tested against chloride salts by Porcayo-Calderon et al. [22,23]. The produced coatings showed remarkable anti-corrosion performance especially at high temperatures (up to 450°C), whereas the uncoated stainless steel 304 substrate experienced severe corrosion. Flame-sprayed Ni20Cr coatings provided good protection against V_2O_5-$NaSO_4$ molten salt mixtures up to 750°C reducing the corrosion rate of the steel substrate by more than 50% compared to the uncoated steel [24]. Gomez-Vidal et al. [25,26] and Raiman et al. [27] furtherly investigated Ni-Cr coatings manufactured by HVOF, air plasma spray (APS), and diamond jet spray processes, respectively, against molten chlorides and carbonates. Their outcomes indicate that protection by the thermally sprayed coatings is a viable approach to extend the usage of carbonates and chlorides for the TES system, allowing to increase the operating temperature up to 700/750°C. Apart from the recalled studies, in the authors’ best knowledge no further contributions on that topic can be found in the devoted literature and many challenges remain unsolved [28]. The present work aims to furtherly investigate the feasibility of compact plasma sprayed coatings of nickel-based alloys against nitrate salts under the working conditions established in TES storage tanks. Compact plasma spray (CPS) has been employed to manufacture Inconel 625 coatings on commercial low-alloyed steel. The CPS consists of a portable plasma spray equipment operating at a maximum power of 2.5 kW and limited working pressure [29]. The reduced requirements allow operating in-situ on the TES components for installation and maintenance operations, preventing moving away from the damaged parts and limiting the shutdown time of the plants.

Materials and Methods

Compact plasma spray system (Sulzer Metco AG, Switzerland), with the compact plasma gun mounted on an Agilus industrial anthropomorphic robot from Kuka was used to deposit Inconel 625 alloy powders onto T22 steel coupons adopting an optimized set of parameters. Oerlikon Mecto Amdry 625 powders (figure 1), having nominal particle size distribution from 90 to 45 μm. The nominal compositions of Inconel 625 and low-grade T22 steel are summarized in the following table.

Table 1. Chemical composition of Inconel 625 powders and T22 steel substrate

Materials	**Chemical Composition (nominal wt. %)**							
	Ni	**Cr**	**Fe**	**Mo**	**Al**	**Nb**	**Ti**	**C**
Amdry 625	bal.	21.5	2.5	9.0	--	3.7	--	--
	Fe	**Cr**	**Si**	**Mo**	**P**	**S**	**Mn**	**C**
T22	bal.	1.92.6	0.5	00.87-1.13	0.03	0.03	0.3-0.6	0.15

Figures 2.a and 2.b report the coupons of uncoated T22 steel and the T22 coated with Inconel 625 powders before the corrosion test in molten salts. Figure 2.c shows the cross-section of the as-sprayed Inconel 625 powders.

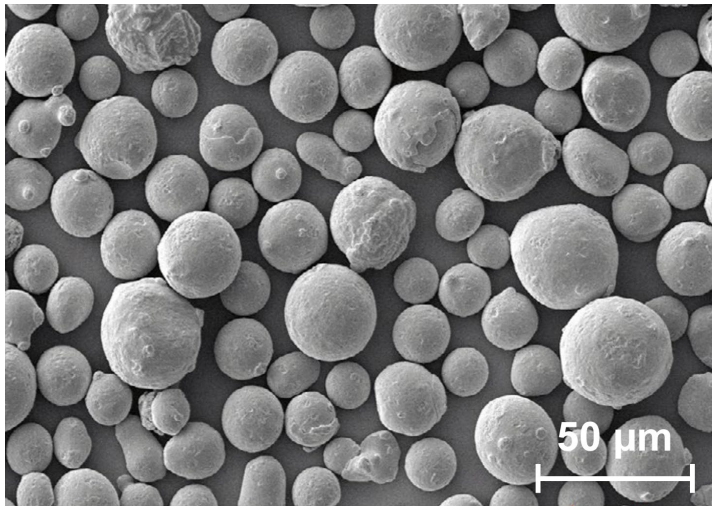

Figure 1. SEM image of Inconel 625 powders (curtesy from Oerlikon Mecto, DSMTS-0085.7 – Nickel Chromium Superalloy (Inconel) Powders, www.oerlikon.com/metco)

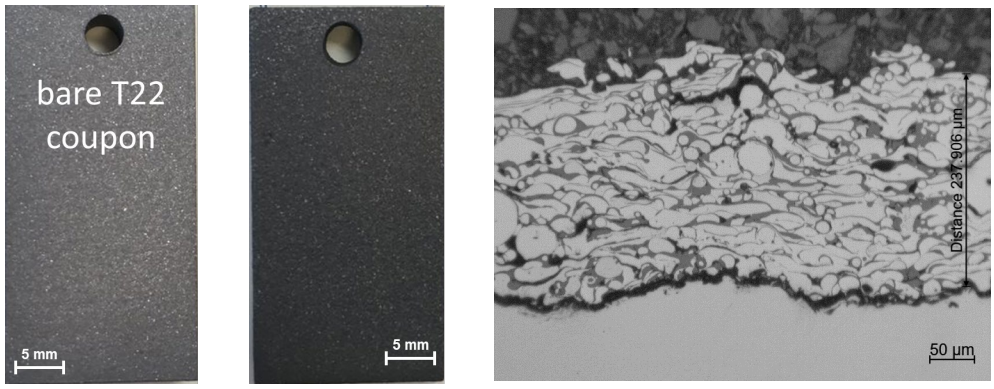

a) b) c)

Figure 2. Uncoated (a) and Inconel 625-coated (b) T22 coupons for the hot corrosion tests; c) cross-section of the coated coupon after the deposition of Inconel 625 powder by CPS system.

A high purity nitrate salts mixture, 60%$NaNO_3$-40%KNO_3, was used as a corrosion medium. This mixture is commonly employed in CSP systems as heat thermal fluid in the power cycle and thermal storage fluid for TES systems.

The coated and uncoated samples were immersed in the molten salts within alumina crucibles and kept at 500°C in a furnace for 24, 72, 168, and 336 hours to assess the corrosion behavior of the Inconel 625 coatings. After the tests, the samples were washed in de-ionized water using ultrasonic cleaning to remove residual traces of salts on their surface. The samples were weighed before and after the tests to evaluate mass gain or loss. The surfaces of the corroded samples were analyzed, after being cleaned from the residuals of the salts, by using an optical and the Hitachi S-3400

(Hitachi, Japan) scanning electron microscope (SEM), equipped with an energy dispersive X-ray microanalysis (EDX), to estimate eventual alterations in the superficial appearance. Samples were, then, cut and mounted in epoxy resin for the subsequent microstructural analysis on the cross-sections. The formation of oxidized layers on the top surfaces of the samples, penetration depth of the corrosion products within the coatings and the substrate, and their chemical compositions were investigated.

Results and Discussion

Uncoated T22 and Inconel 625-coated T22 coupons were tested against a nitrate salts mixture at 500°C. Figure 3 shows the surface of the tested coupons at different exposure times. Bare T22 steel showed a progressive degradation with the increasing of time. After 72 hours, the surface, immersed inside the molten salts pool, presents evident traces of degradation. The oxide layer, which should be hematite iron oxide (Fe_2O_3), appears dense and compact and is uniform across the exposed surface. With the increase of time, the oxide layer begins degrading. After 336 hours, indeed, local traces of the erosion are visible: the oxide layer loses its integrity and breaks, exposing the underlying material, which probably consists of other species of iron oxide, that are less resistant to the aggressive action of the salts. Cyclic formation, growth, and spallation of the primary oxide layer represent the mechanism by which the corrosion propagates within the T22 steel. The surface of the steel, which was not directly in contact with the liquid salts but was exposed to the high temperatures, also experienced an oxidation reaction. Inconel-coated samples, conversely, at a preliminary observation did not show remarkable signs of corrosion and the coating appears to retain its integrity regardless of the time of exposure to the molten salts. The tested coupon differs from the as-sprayed sample for a slight change in the surface coloration, probably due to the reaction of the constituents of the nickel alloy, iron, and chromium in particular, with the environment.

a) b) c) d) e) f)

Figure 3. Images of the surface of the coupons after the corrosion tests at different times of exposure: uncoated T22 after three (a), seven (b) and 14 days (c) and Inconel 625-coated T22 after three (d), seven (e) and 14 days (f). Sub-figures c, e (on the right), and f (on the left) also show the relative coupon before the hot corrosion test for comparison purpose

Figure 4 reports the mass variation for the surface unit for the uncoated and coated coupons. T22 steel showed an increasing mass gain with the increasing exposure time, related to the growth of the superficial oxide layer, which ranges between 15 and 27 μm after 24 hours, while it reaches approximately 60 μm after 336 hours. It is worthy of noting that gravimetric analysis showed that the mass gain after 168 hours is higher than the ones measured at the maximum testing exposure time, which are 8.7 and 8.35 mg/cm^2, respectively. A reduction in the mass gain rate is expected due to the protective action exerted by the thicker oxide layer with respect to the early stage of the corrosion where the steel has not yet formed a protective layer and it is in contact directly with the

salt or it is covered by a very thin film of oxide [10]. To assess if the observed variation is a trend or a local oscillation, tests with longer exposure time could be needed.

Inconel 625-coated steel showed a mass loss during exposure to the molten salts. Mass loss in bulk Inconel 625 is expected due to the dissolution of the oxides (in particular chromium oxide) within the molten salts [30]. However, it is very limited at the testing temperatures adopted in the present work. The value measured, indeed, is three orders of magnitude higher than the value reported in the literature [30]. The discrepancy between bulk and coating can be ascribed to the progressive erosion of the coating with the increasing exposure time: Inconel 625 coating indeed passed from approximately 240 µm in as-sprayed conditions (see figure 2.c), to 110 µm after 336 hours (as visible in figure 9). It will be discussed later in the manuscript.

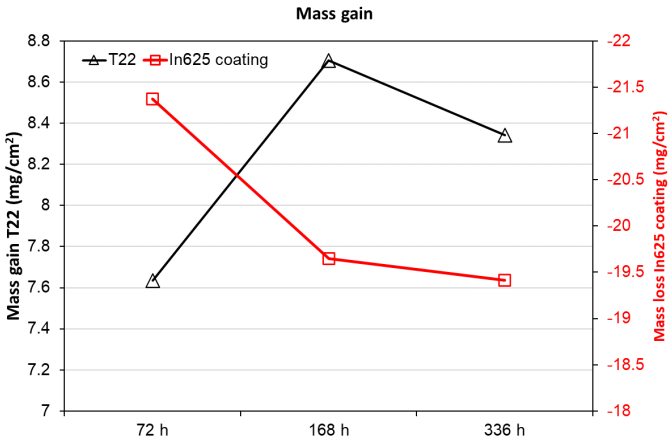

Figure 4. Mass variations of uncoated and Inconel 625-coated T22 coupon after hot corrosion test at different times of exposure to the molten salts.

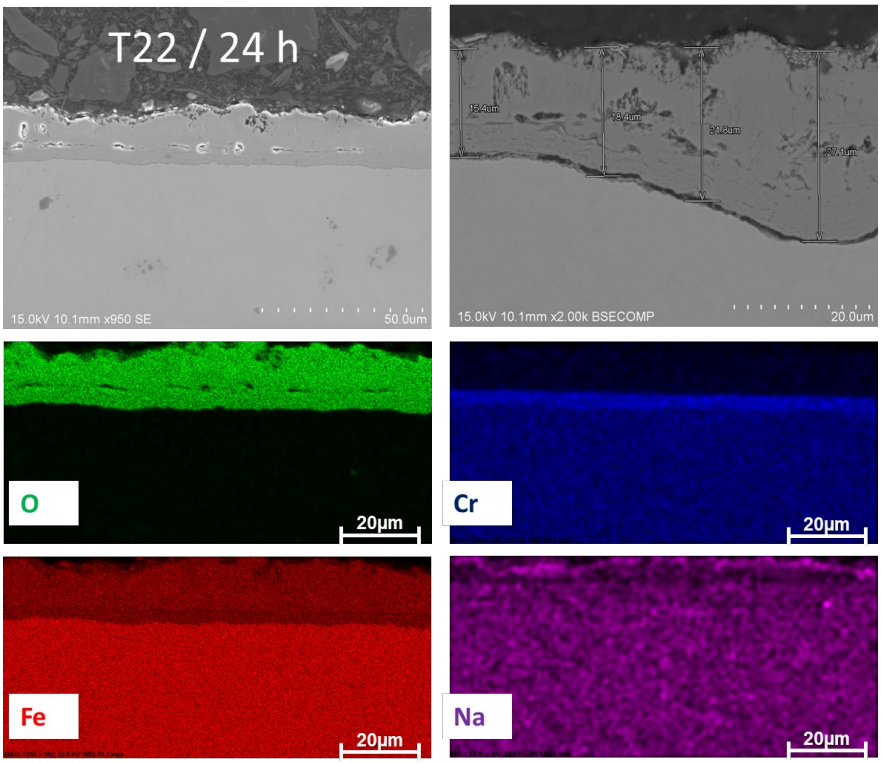

Figure 5. Cross-section and EDX maps of the uncoated T22 specimen after 24 hours of exposure.

Figures 5 and 6 show the cross-section and the EDX analysis of the uncoated T22 after 24 and 336 hours of exposure, respectively. As mentioned previously, the main corrosion product consists of an iron oxide layer. The layer has been claimed to be formed by hematite on the external layer in

direct contact with the nitrates and by magnetite on the internal layer in contact with the steel substrate [31]. At the interface with the substrate, a layer rich in chromium formed resulting in a depletion of the bulk steel near the surface exposed to the salts. The hematite layer is usually less compact and less adherent to the underlying layer. The porosity in the outer oxide promotes the penetration of the corrosion medium inside the oxide layer, with the consequent spallation of the layer and the progression of the corrosion of the steel (see figure 6). Only a few traces of sodium or potassium have been detected on the surface and within the oxide coating.

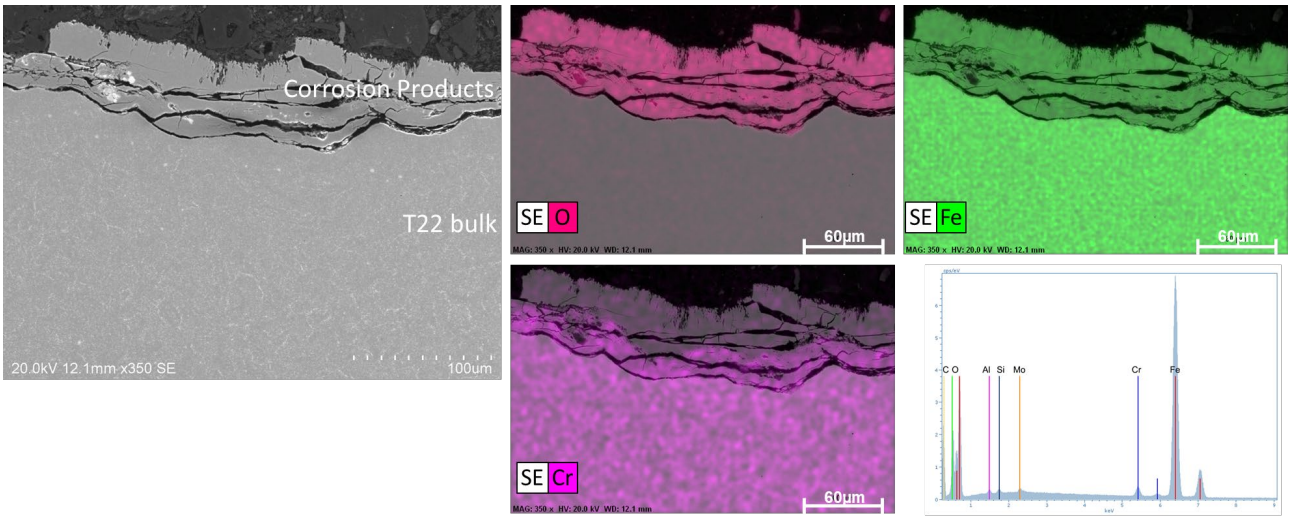

Figure 6. EDX maps of the cross-section of the uncoated T22 specimen after 336 hours of exposure.

Figures 7, 8, and 9 show the cross-section, the surface, and the EDX analysis of the Inconel 625-coated T22 steel after 24 and 336 hours of exposure. After one day, no remarkable signs of corrosion are visible on the coating: thin oxide scales formed on the surface composed of sodium and iron, probably Na_2FeO_2 [30,32]. The dissolution of these scales in the molten salts has been indicated as a reason contributing to the weight loss also in the Inconel 625 bulk [30]. Traces of sodium have been also observed between the splats in the region rich in chromium, niobium, and oxygen. After 24 hours, the penetration of sodium inside the coating is limited and it does not weaken the integrity of the coating itself.

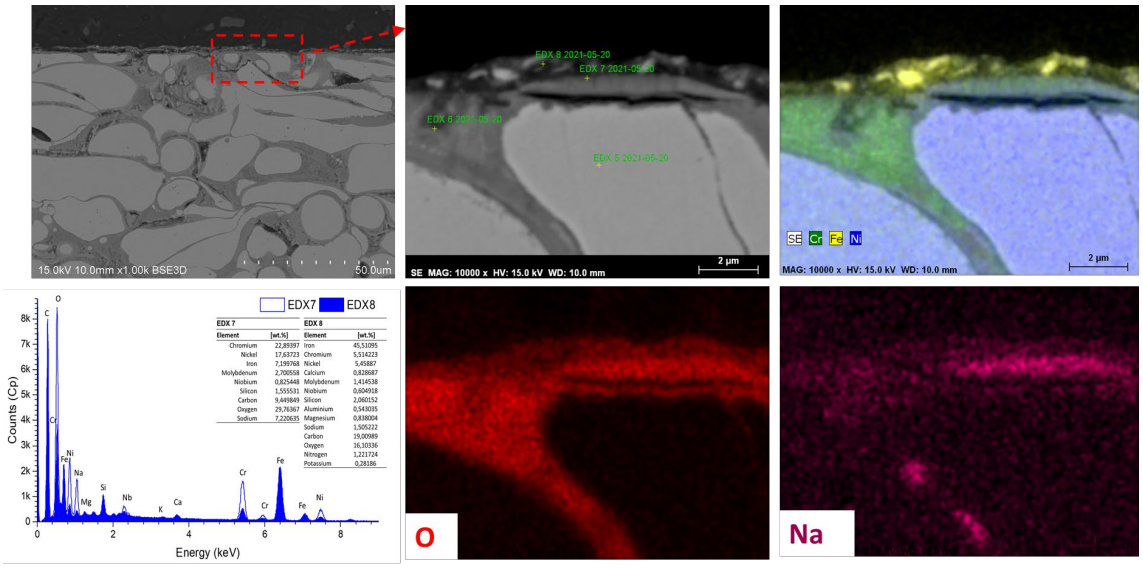

Figure 7. EDX maps of Inconel 625-coated T22 steel cross-section after 24 hours of exposure.

After 336 hours, the coating shows evident signs of the progression of corrosion. On the surface, the main phase consists of NiO nickel oxide, while a secondary phase concentrate in the region between the nickel particle is composed of niobium and chromium, precipitated at the particle boundaries after the plasma spraying (see also figure 2.c), and sodium, which was found a high concentration (see figure 8). The sodium also penetrates deeper within the coating with the increasing exposure time up to more than half of the actual coating through the pores between the sprayed particles (see figure 9). As mentioned before, the diffusion of the corrosive agent and formation of corrosion product inside the coating led to a lack of cohesion of the sprayed particles and a loss in structural integrity: the coating delaminates and part of it is lost in the early phase of the test, up to 168 hours, and it remains roughly constant up to 336 h. It could be the reason for the reduction in the coating thickness measured after fourteen days test and the mass loss higher than that observed in the Inconel 625 bulk [30]. The formation of uniform chromium oxide at the interface between the steel substrate and the coating was also observed. Chromium oxide is a stable compound at the operative conditions adopted and exerts a protective action for the underlying steel, which did not experience significant degradation, retaining its original composition and integrity.

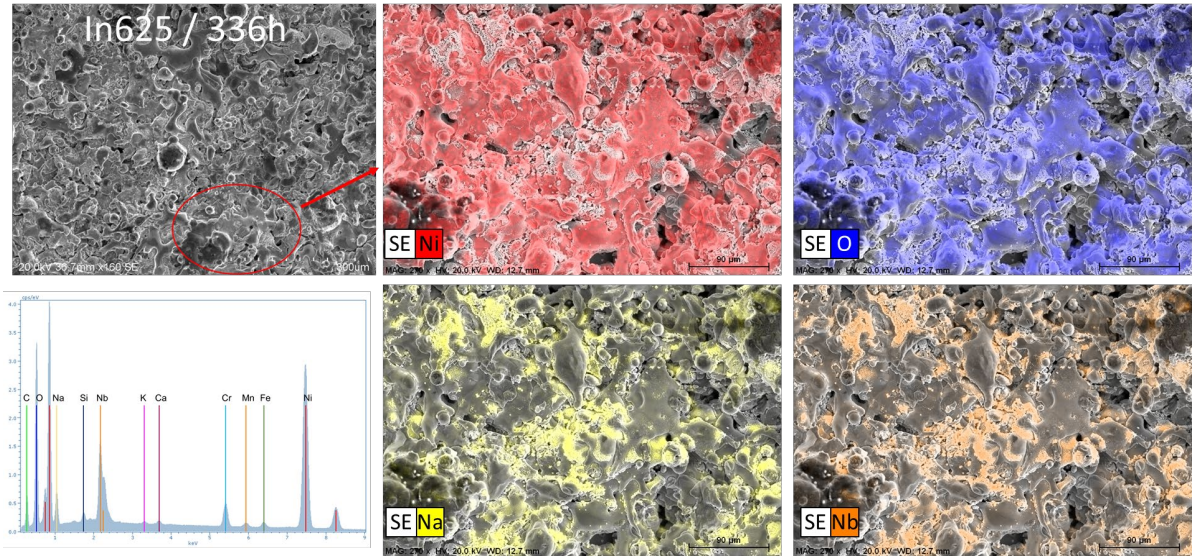

Figure 8. EDX map of the surface of Inconel 625 coated coupon after 336 hours of exposure.

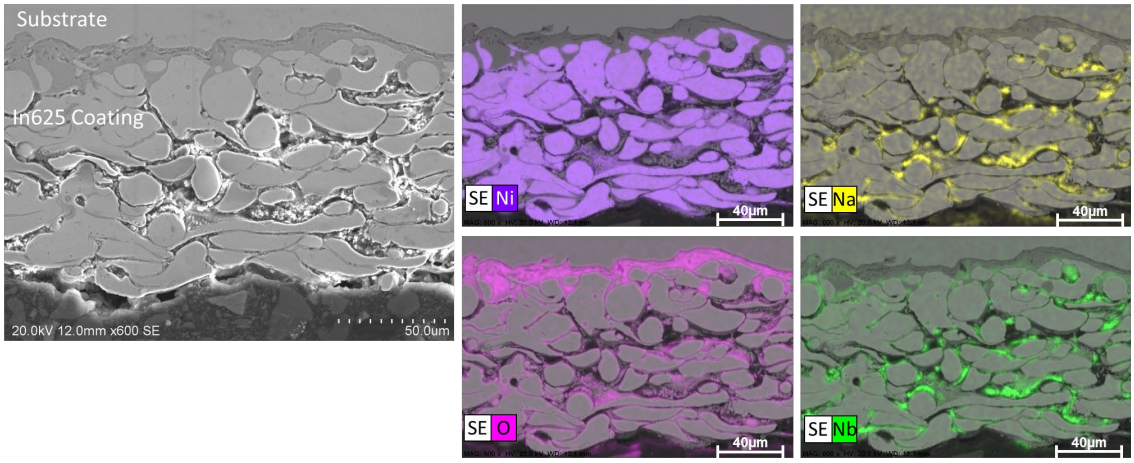

Figure 9. EDX analysis of Inconel 625-coated T22 after 336 of exposure.

Conclusions

Inconel 625 coating, deposited on T22 steel substrate by using compact plasma spray process, was tested against molten salts at 500°C for different exposure time, namely 24, 72, 168, and 336 hours.

By analyzing the outcomes from the experimental campaign, the following conclusions can be drawn:

- T22 Steel was severely affected by the exposure to the molten salts. The surface in contact with the salts show evident signs of extended corrosion, with spots correspondent to the localized fracture of the oxidized layer
- T22 tends to form a dense oxidized layer mainly formed by Fe_2O_3 and Fe_3O_4 compounds. Slight traces of sodium and potassium have been observed on the corroded surface.
- Inconel 625 coating behaves well when exposed to molten salts. No damages have been observed on the T22 substrate, which retains its composition. Corrosion products, consisting of Na and O compounds, were found inside the coating, forming within the pores between the particle splats resulting from the deposition process. Inter-splat corrosion could lead to the weakening and potential erosion of the coatings
- Corrosion products propagate deeper inside the Inconel coating with increasing the exposure time, from a few microns after 24 h up to half the thickness after 336h

Acknowledgments

This project received funding from the European Union's Horizon 2020 research and innovation programme under the Marie Skłodowska-Curie grant agreement No. 754382. The authors also wish to thank "Comunidad de Madrid" and European Structural Funds for their financial support to the ACES2030-CM project (S2018/EMT-4319).

References

[1] F. Rovense, M. Perez, M. Amelio, V. Ferraro, N. Scornaienchi, Feasibility analysis of a solar field for a closed unfired Joule-Brayton cycle, Int J Heat Technol 35 (2017) 166–71.

[2] F. Rovense, M.Á. Reyes-Belmonte, M. Romero, J. González-Aguilar, Thermo-economic analysis of a particle-based multi-tower solar power plant using unfired combined cycle for evening peak power generation, Energy 240 (2022) 122798.

[3] M. Walczak, F. Pineda, Á.G. Fernández, C. Mata-Torres, R.A.Escobar, Materials corrosion for thermal energy storage systems in concentrated solar power plants, Renew Sustain Energy Rev 86 (2018) 22–44.

[4] M. Sarvghad, S. Delkasar Maher, D. Collard, M. Tassan, G. Will, T.A. Steinberg, Materials compatibility for the next generation of Concentrated Solar Power plants, Energy Storage Mater 14 (2018)179–98.

[5] S. Bell, T. Steinberg, G.Will, Corrosion mechanisms in molten salt thermal energy storage for concentrating solar power, Renew. Sustain. Energy Rev. 114 (2019)109328.

[6] M.T. Islam, N. Huda, A.B. Abdullah, R.Saidur, A comprehensive review of state-of-the-art concentrating solar power (CSP) technologies Current status and research trends, Renew Sustain Energy Rev 91 (2018) 987–1018.

[7] K. Vignarooban, X. Xu, A. Arvay, K. Hsu, A.M. Kannan, Heat transfer fluids for concentrating solar power systems – A review, Appl Energy 146 (2015) 383–96.

[8] S. Goods, R. Bradshaw, M. Prairie, J. Chavez, Corrosion of stainless and carbon steels in molten mixtures of industrial nitrates. Sandia National Lab, Livermore, CA (United States) 1994.

[9] A.G. Fernández, H. Galleguillos, E. Fuentealba, F.J. Pérez, Corrosion of stainless steels and low-Cr steel in molten $Ca(NO_3)_2$–$NaNO_3$–KNO_3 eutectic salt for direct energy storage in CSP plants, Sol Energy Mater Sol Cells 141 (2015) 7–13.

[10] A.G. Fernández, M. Cortes, E. Fuentealba, F.J. Pérez, Corrosion properties of a ternary nitrate/nitrite molten salt in concentrated solar technology, Renew Energy 80 (2015) 177–83.

[11] M. Gonzalez, U. Nithiyanantham, E. Carbó-Argibay, O. Bondarchuk, Y. Grosu, A. Faik, Graphitization as efficient inhibitor of the carbon steel corrosion by molten binary nitrate salt for thermal energy storage at concentrated solar power, Sol Energy Mater Sol Cells 203 (2019) 110172.

[12] W. Ding, A. Bonk, J. Gussone, T. Bauer, Electrochemical measurement of corrosive impurities in molten chlorides for thermal energy storage, J Energy Storage 15 (2018) 408–14.

[13] H. Singh, D. Puri, S. Prakash, T.K. Ghosh, Hot corrosion of a plasma sprayed Ni3Al coating on a Ni-base superalloy, Mater Corros 58 (2007) 857–66.

[14] A. Agüero, F.J. García de Blas, M.C. García, R. Muelas, A. Román, Thermal spray coatings for molten carbonate fuel cells separator plates, Surf Coatings Technol 146–147 (2001) 578–85.

[15] A. Agüero, Progress in the development of coatings for protection of new generation steam plant components, Energy Mater 3 (2008) 35–44.

[16] A. Astarita, S. Genna, C. Leone, F.M.C. Minutolo, F. Rubino, A. Squillace, Study of the Laser Remelting of a Cold Sprayed Titanium Layer, Procedia CIRP 33 (2015) 452–7.

[17] F. Rubino, P. Ammendola, A. Astarita, F. Raganati, A. Squillace, A. Viscusi, et al. An Innovative Method to Produce Metal Foam Using Cold Gas Dynamic Spray Process Assisted by Fluidized Bed Mixing of Precursors, Key Eng Mater 651–653 (2015) 913–8.

[18] V. Paradiso, F. Rubino, F. Tucci, A. Astarita, P. Carlone, Thermo-mechanical modeling of laser treatment on titanium cold-spray coatings, AIP Conf. Proc. 1960 (2018) 100011.

[19] F. Rubino, A. Astarita, P. Carlone, S. Genna, C. Leone, F. Memola Capece Minutolo, et al. Selective Laser Post-Treatment on Titanium Cold Spray Coatings, Mater Manuf Process 31 (2016) 1500–6.

[20] F. Rubino, V. Paradiso, A. Astarita, P. Carlone, A. Squillace, Advances in Titanium on Aluminium Alloys Cold Spray Coatings, in: P. Cavaliere (Eds.), Cold-Spray Coatings, Springer International Publishing, Cham, 2018, pp. 225–49.

[21] A. Viscusi, A. Astarita, R. Della Gatta, F. Rubino, A perspective review on the bonding mechanisms in cold gas dynamic spray, Surf Eng 35 (2019) 743–71.

[22] J. Porcayo-Calderon, O. Sotelo-Mazon, V.M. Salinas-Bravo, C.D. Arrieta-Gonzalez, J.J. Ramos-Hernandez, C. Cuevas-Arteaga, Electrochemical Performance of Ni20Cr coatings applied by combustion powder spray in $ZnCl_2$-KCl molten salts, Int J Electrochem Sci 7 (2012) 1134–48.

[23] J. Porcayo-Calderón, O. Sotelo-Mazón, M. Casales-Diaz, J.A. Ascencio-Gutierrez, V.M. Salinas-Bravo, L. Martinez-Gomez, Electrochemical study of Ni20Cr coatings applied by HVOF Process in $ZnCl_2$-KCl at high temperatures, J Anal Methods Chem 2014 (2014) 503618.

[24] A.J.L. Marulanda, Corrosión en sales fundidas de un acero recubierto mediante rociado térmico por llama, Prospectiva 12 (2014) 15.

[25] J.C. Gomez-Vidal, Corrosion resistance of MCrAlX coatings in a molten chloride for thermal storage in concentrating solar power applications, Npj Mater Degrad 1 (2017) 1–8.

[26] J.C. Gomez-Vidal, J. Noel, J. Weber, Corrosion evaluation of alloys and MCrAlX coatings in molten carbonates for thermal solar applications, Sol Energy Mater Sol Cells 157 (2016) 517–25.

[27] S.S. Raiman, R.T. Mayes, J.M. Kurley, R. Parrish, E. Vogli, Amorphous and partially-amorphous metal coatings for corrosion resistance in molten chloride salt, Sol Energy Mater Sol Cells 201 (2019) 110028.

[28] F. Rubino, P. Poza, G. Pasquino, P. Carlone, Thermal Spray Processes in Concentrating Solar Power Technology, Metals 11 (2021) 1377.

[29] A. Rico, A. Salazar, M.E. Escobar, J. Rodriguez, P. Poza, Optimization of atmospheric low-power plasma spraying process parameters of Al_2O_3-50wt%Cr_2O_3 coatings, Surf Coatings Technol 354 (2018) 281–96.

[30] A. Soleimani Dorcheh, R.N. Durham, M.C. Galetz, Corrosion behavior of stainless and low-chromium steels and IN625 in molten nitrate salts at 600 °C, Sol Energy Mater Sol Cells 144 (2016) 109–16.

[31] A.G. Fernández, M.I. Lasanta, F.J. Pérez, Molten Salt Corrosion of Stainless Steels and Low-Cr Steel in CSP Plants, Oxid Met 78 (2012) 329–48.

[32] X. Ou, Z. Sun, M. Sun, D. Zou, Hot-corrosion mechanism of Ni-Cr coatings at 650°C under different simulated corrosion conditions, J China Univ Min Technol 18 (2008) 444–8.